Immunity
Article

Dynamics of Neutrophil Migration in Lymph Nodes during Infection

Tatyana Chtanova,[1,3] Marie Schaeffer,[1,3] Seong-Ji Han,[1,3] Giel G. van Dooren,[2] Marcelo Nollmann,[1] Paul Herzmark,[1] Shiao Wei Chan,[1] Harshita Satija,[1] Kristin Camfield,[1] Holly Aaron,[1] Boris Striepen,[2] and Ellen A. Robey[1,*]
[1]Department of Molecular and Cell Biology, Life Sciences Addition, University of California, Berkeley, CA 94720, USA
[2]Center for Tropical & Emerging Global Diseases and Department of Cellular Biology, University of Georgia, Paul Coverdell Center, Athens, GA 30602, USA
[3]These authors contributed equally to this work
*Correspondence: erobey@berkeley.edu
DOI 10.1016/j.immuni.2008.07.012

SUMMARY

Although the signals that control neutrophil migration from the blood to sites of infection have been well characterized, little is known about their migration patterns within lymph nodes or the strategies that neutrophils use to find their local sites of action. To address these questions, we used two-photon scanning-laser microscopy to examine neutrophil migration in intact lymph nodes during infection with an intracellular parasite, *Toxoplasma gondii*. We found that neutrophils formed both small, transient and large, persistent swarms via a coordinated migration pattern. We provided evidence that cooperative action of neutrophils and parasite egress from host cells could trigger swarm formation. Neutrophil swarm formation coincided in space and time with the removal of macrophages that line the subcapsular sinus of the lymph node. Our data provide insights into the cellular mechanisms underlying neutrophil swarming and suggest new roles for neutrophils in shaping immune responses.

INTRODUCTION

Neutrophils are the most abundant nucleated cell in the blood and play a crucial role in immune responses to pathogens. Neutrophils are best known for their role in phagocytosis and killing of extracellular bacteria; however, they can provide protection against a diverse set of pathogens, and do so by performing a variety of different functions (reviewed in Appelberg [2007] and Nathan [2006]). These functions include tissue remodeling, antigen presentation, recruiting other blood cells, and polarizing T cell responses (Beauvillain et al., 2007; Megiovanni et al., 2006; Pesce et al., 2008; Tvinnereim et al., 2004). For example, neutrophils play an important protective role during infection with the intracellular protozoan parasite *Toxoplasma gondii* (Bennouna et al., 2003; Bliss et al., 2001; Denkers et al., 2004; Sayles and Johnson, 1996) in spite of the fact that the parasite is relatively resistant to killing by neutrophils (Channon et al., 2000; Nakao and Konishi, 1991b). There is evidence that the protective effect of neutrophils during *Toxoplasma* infection is due in part to the production of interleukin-12 (IL-12) by neutrophils and the subsequent shaping of the adaptive immune response (Bennouna et al., 2003). However, the precise roles of neutrophils during infection remain poorly understood.

Neutrophils are produced in the bone marrow, circulate in the blood, and are rapidly recruited to sites of infection in response to a variety of chemoattractants produced by inflamed tissues (reviewed in Baggiolini [1998] and Scapini et al. [2000]). A number of studies have shown that neutrophils can also traffic to lymph nodes in response to infection (Abadie et al., 2005; Maletto et al., 2006; Pesce et al., 2008), raising the possibility that neutrophils may modulate immune responses within lymph nodes. One powerful tool for investigating the function of cells within lymph nodes is two-photon scanning-laser microscopy (TPSLM), an imaging method that provides dynamic information about cell migration and interactions within tissue samples (reviewed in Bousso and Robey [2004], Germain et al. [2006], Sumen et al. [2004], and Cahalan and Parker [2008]). Thus far, this approach has been primarily used to examine responses to model antigens by T and B cells and is just beginning to be applied in the setting of infection and to examine immune responses of nonlymphoid cells (Egen et al., 2008; Zinselmeyer et al., 2008).

Despite their abundance, physiological importance, and clear indications that they can traffic to lymph nodes during infection, we know very little about what neutrophils do in the lymph node. Do neutrophils work individually, or in groups? What are the cues that guide neutrophil migration within lymph nodes? What impact do neutrophils have on other cell types in lymph nodes? Here, we addressed these questions using TPSLM and a *Toxoplasma gondii*-mouse infection model. We found that neutrophils accumulate in the subcapsular sinus of the draining lymph node after infection and form both small, transient and large, persistent swarms via a highly coordinated migration pattern. We provided evidence that cooperative action of neutrophils and parasite egress from host cells can trigger swarm formation and that neutrophil swarms lead to the removal of macrophages that line the subcapsular sinus of the lymph node. These results provide insight into the cellular mechanisms that lead to neutrophil swarms and suggest new potential functions for neutrophils in lymph nodes.

RESULTS

An Experimental Model to Examine Neutrophil Migration in Lymph Nodes

In order to examine the behavior of neutrophils in lymph nodes during infection, we infected mice with the intracellular

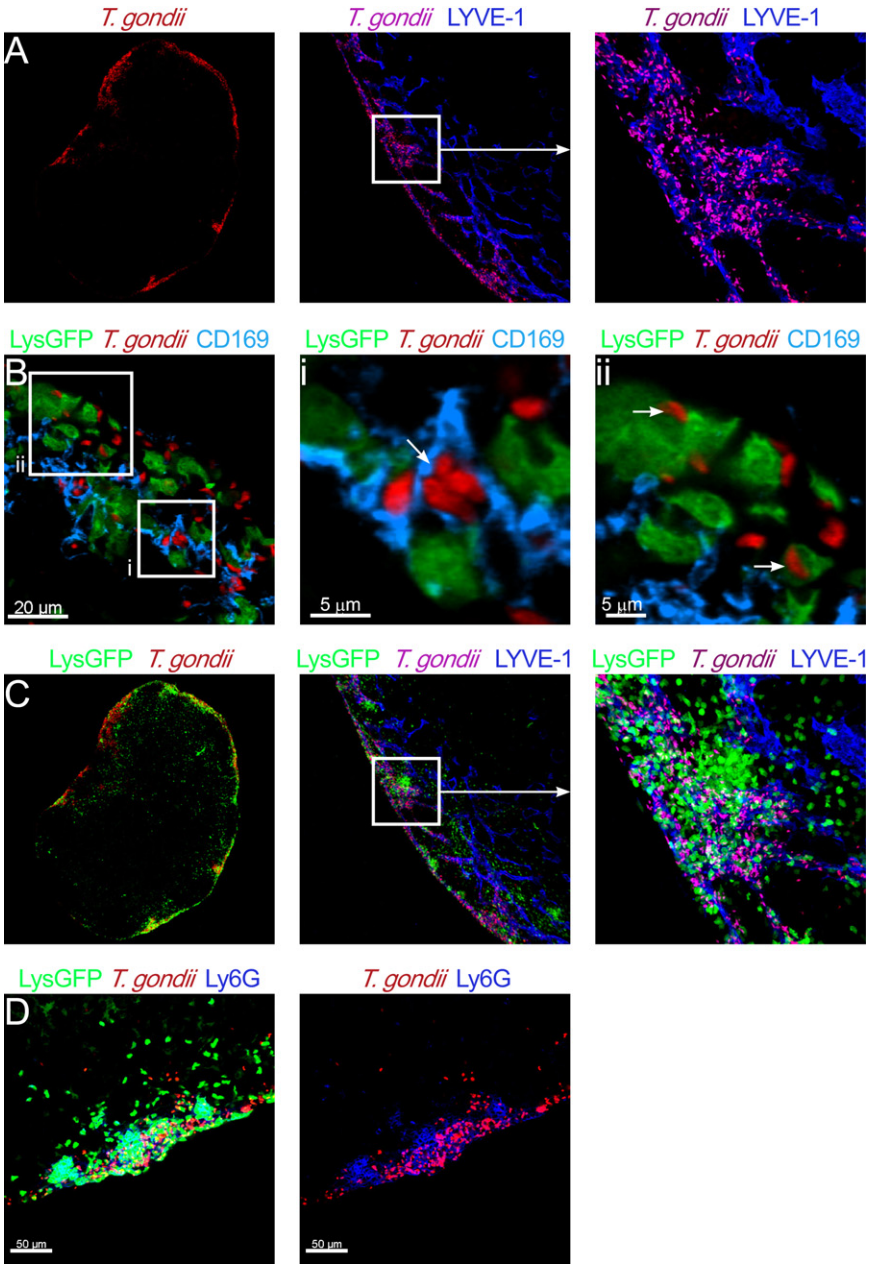

Figure 1. Location of *T. gondii* Relative to Lymphatics, CD169 Macrophages, and Neutrophils in Draining Lymph Nodes after Ear-Flap Infection

(A) A 20 μm frozen section of a draining lymph node 4 hr after an earflap injection with RFP (red) parasites. The middle and right panels show staining with LYVE-1 (blue) used for visualization of the lymphatic system. The right panel shows a high-magnification image.

(B) A 20 um frozen section of a draining lymph node from a mouse bearing the LysGFP reporter (green) 4 hr after an earflap injection with RFP (red) parasites and stained with CD169 (blue) to label subcapsular sinus macrophages. The middle panel shows an enlarged area with parasites inside $CD169^+$ cells. The right panel shows an enlarged area with intact parasites inside neutrophils.

(C) Same samples as in (A) showing signal from the LysGFP reporter (green).

(D) Clusters of LysGFP high cells (green) (left panel) stain positive for the neutrophil marker Ly6G (blue). The right panel shows the same image without the LysGFP signal.

protozoan parasite *Toxoplasma gondii*. After injection of live fluorescent parasites into the earflap, parasites can be found within 1 hr in the subcapsular sinus of the draining lymph node in association with $LYVE1^+$ lymphatic vessels (Figure 1A). Many parasites are found within the $CD169^+$ macrophages that line the subcapsular sinus (Figure 1B, middle), a distribution similar to that seen with other particulate antigens, such as viruses and immune complexes (Carrasco and Batista, 2007; Junt et al., 2007; Phan et al., 2007).

In order to track neutrophils relative to red fluorescent protein (RFP)-labeled parasites, we used reporter mice in which GFP is under the control of the lysozyme M promoter (lysGFP) (Faust et al., 2000). Although this reporter is also expressed by macrophages and a subset of dendritic cells, the vast majority of the GFP^{hi} cells in the lymph nodes at 1–5 hr after infection are neutrophils, on the basis of their cell-surface phenotype ($Ly6G^{hi}CD11b^{hi}CD11c^{lo}$) (Rydstrom and Wick, 2007; Sasmono et al., 2007) (see Figure S1A available online). Neutrophil recruitment to the draining lymph nodes occurred rapidly and was dependent on the Toll-like receptor (TLR)-interleukin-1 receptor (IL-1R) adaptor protein, MyD88 (Figure S1A). Interestingly, many neutrophils were associated with $LYVE1^+$ lymphatic vessels (Figure 1C). This is consistent with the possibility that neutrophils entered the lymph node via lymphatics, as has been reported previously (Abadie et al., 2005; Maletto et al., 2006). We also detected neutrophils within blood vessels of infected lymph nodes (data not shown), suggesting that neutrophils may enter lymph nodes via both blood and lymph.

At early times after infection, neutrophils contained proportionally more parasites compared to macrophages and dendritic cells (Figure S1B). Although phagocytic destruction of pathogens is one protective mechanism used by neutrophils, the parasites inside neutrophils appear intact (Figure 1B, right). This is consistent with evidence that *T. gondii* can divide in vitro in human neutrophils (Channon et al., 2000; Nakao and Konishi, 1991b) and indications that the protective effects of neutrophils during *T. gondii* infection are due to immunoregulation rather than direct killing mechanisms (Bennouna et al., 2003; Bliss et al., 2001; Denkers et al., 2004; Sayles and Johnson, 1996).

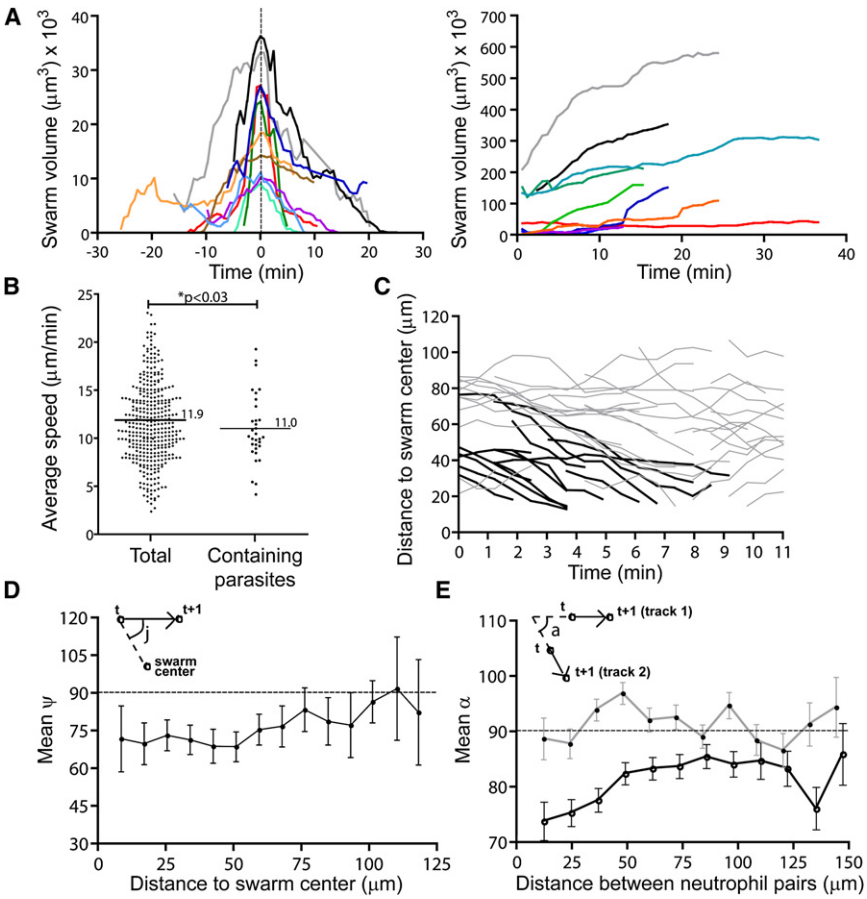

Figure 2. Neutrophil Migration and Swarm Formation in Infected Lymph Nodes

Mice expressing a macrophage and neutrophil transgenic reporter (LysGFP) were infected in the ear flap and draining lymph nodes removed at 2–5 hr after infection were imaged with TPSLM. As shown in (A), neutrophils form transient (left panel) and persistent (right panel) swarms in intact lymph nodes. The volumes of individual swarms were plotted versus elapsed imaging time. Transient swarms were all <4 × 10^4 μm^3, corresponding to ~150 cells on the basis of an average volume of a single neutrophil from these runs (275 μm^3). (B) shows the quantitation of neutrophil motility. Each point represents the average speed for an individual track of a neutrophil outside of a swarm. Data for neutrophils that contained parasites were plotted on the right. (C) shows distance to swarm center versus time. Each line represents an individual track. Solid black lines correspond to neutrophils that eventually enter a swarm. Gray lines correspond to tracks of neutrophils that do not enter the swarm. (D) shows the plot of the mean "directionality angle" or psi for a run in which swarms formed. Psi values were binned on the basis of the distance of the cell to the swarm center, and the mean values are plotted versus the distance to swarm center. The dashed line indicates the value expected for random migration (90 degrees). Values less than 90 degrees indicate directed migration toward the swarm center. Values were expressed as mean ± standard error. The confidence interval over all distances is 73–77 degrees, and the p value for the probability that the mean distribution is 90 degrees is 10^{-40}. (E) shows coordinated migration during swarm formation. Alpha values were binned on the basis of the distance between cell pairs and plotted versus the distance between pairs. The solid black line represents the values for a run with a swarm. The gray line represents the values for a run with no obvious swarms. Values were expressed as mean ± standard error. The confidence interval for the run with a swarm over all distances is 77–83 degrees, and the p value for the probability that the mean distribution is 90 degrees is 10^{-5}. The confidence interval for the run without a swarm over all distances is 88–93 degrees, and the p value for the probability that the mean distribution is 90 degrees is 0.3.

Neutrophils Form Dynamic Swarms in the Subcapsulary Sinus of the Lymph Node

Analysis of tissue sections of lymph nodes from infected mice showed that reporter-positive cells formed large clusters along the subcapsular sinus, and those clusters generally coincided with the location of parasites (Figures 1C and 1D). Virtually all of the reporter bright cells in the subcapsular sinus (SCS) region of the lymph node express Ly6G (Figure 1D), consistent with flow-cytometric analysis (Figure S1A) and confirming their identity as neutrophils.

To examine the dynamics of neutrophil cluster formation and the relationship of cluster formation to infection, we examined intact draining lymph nodes of lysGFP reporter mice infected with RFP parasites using TPSLM. Visual inspection of time-lapse imaging data revealed the striking dynamics of neutrophil swarm formation (Figure 2A and Movies S1, S2, and S3). Some swarms, which we term transient swarms, grew by rapid, large-scale, coordinated migration of neutrophils into the swarm and then quickly dissolved as neutrophils migrated out to join nearby growing swarms (Figure 2A and Movies S1 and S2). Transient swarms formed and dispersed over a period of 10–40 min (mean duration 20 min) and remained relatively small (<4 × 10^4 μm^3, corresponding to ~150 neutrophils). We also noted a distinct type of swarm, which we term persistent swarms, that grew throughout the imaging period (up to 38 min) both by continued migration of neutrophils into the swarm and by merging with nearby smaller swarms (Figure 2A and Movie S3). Persistent swarms tended to be large and occasionally grew to fill the entire imaging volume (>6 × 10^5 μm^3). The relationship between the size and persistence of the swarms is consistent with the notion that neutrophils themselves generate signals that induce swarming and that, once swarms reach a certain size, they produce a large signaling center that can overwhelm competing nearby signals.

Out of a total of 40 runs representing ~20 hr of cumulative imaging time, we observed 30 swarms, of which 16 were transient. We also observed neutrophil recruitment and swarming behavior in lymph nodes after earflap infection with *Listeria monocytogenes* (data not shown). This indicates that swarming is not unique to *T. gondii* infection but may be a more general response to infection. Although we occasionally observed neutrophil swarms in uninfected lymph nodes (two persistent and zero transient swarms seen in 14 runs), these were infrequent compared to infected lymph nodes. This, together with the clear correlation

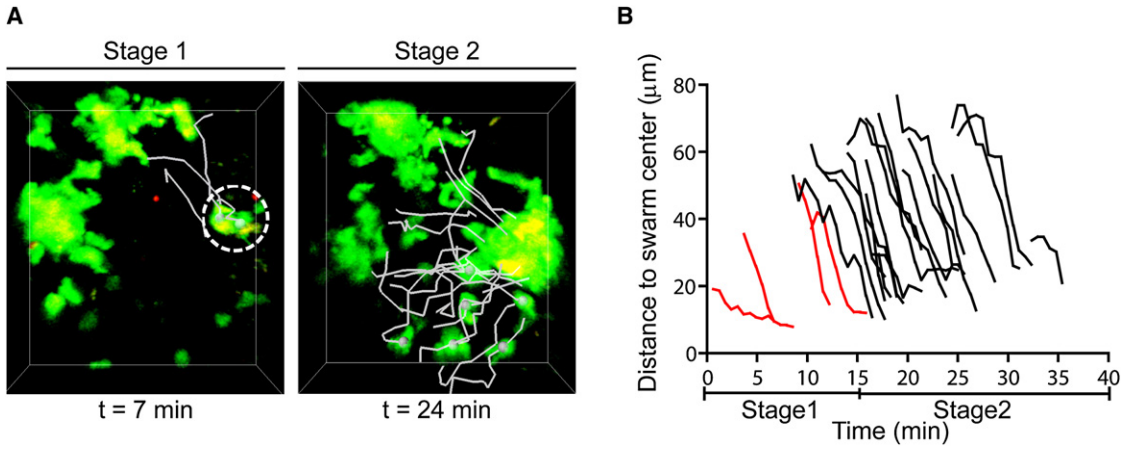

Figure 3. Neutrophil Swarm Formation Can Occur in Two Temporal Stages

(A) Left panel shows a time point during stage 1 with the tracks of early arriving neutrophils depicted as white lines. The right panel shows a time point during stage 2 with the tracks of late-arriving neutrophils depicted as white lines.

(B) Distance to swarm center versus time for the tracks of neutrophils that enter the swarm. The tracks in red correspond to early-arriving neutrophils (stage 1), and the tracks in black correspond to late-arriving neutrophils (stage 2).

between neutrophil recruitment and infection seen from analysis of tissue sections and flow cytometry (Figure 1 and Figure S1), indicates that most neutrophil swarms form as a consequence of infection.

Quantitation of Directed, Coordinated Migration by Neutrophils

To relate neutrophil migration patterns to swarm formation, we tracked individual neutrophils before they entered swarms and during migration without swarming (Figures 2B–2E and Movies S4 and S5). Neutrophils that were not in swarms migrated with average speeds of 11.9 μm/min, substantially faster than a recent report of neutrophil migration in the footpad (Zinselmeyer et al., 2008) but similar to that of naive T cells in intact lymph nodes (Miller et al., 2002 and data not shown). Neutrophils containing parasites migrated only slightly more slowly that those that did not contain parasites (Figure 2B).

In principle, swarms could form either by directed migration or by random migration and retention of cells at sites where swarms were growing, two possibilities that can be distinguished by dynamic imaging. Visual inspection of time-lapse runs in which neutrophil swarms were forming showed large-scale directed migration of neutrophils into swarm center (Movies S1, S2, and S3). To quantitate this directional migration during swarm formation, we measured the distance of neutrophils to the swarm center and plotted the changes in this distance for individual tracks over time. These analyses confirmed that individual neutrophils moved persistently toward the swarm over time, indicative of directed migration (Figure 2C). Persistent movement toward the swarm centers could be seen even when neutrophils were >70 μm away from the swarm center. As an alternative method for quantitating directed migration, we also calculated the angle (psi) defined by the migration trajectory vector and the vector between initial neutrophil position and swarm center and plotted the average psi as function of distance to swarm center (Figure 2D). The mean value for psi should be 90 degrees for random movement, and less than 90 degrees for directed migration into swarms. We found that mean psi was markedly less than 90 degrees even for cells at distances >75 μm away from the swarm center. Together, these analyses indicate that the growth of swarms occurs by large-scale directed migration of neutrophils toward swarm centers.

We noted that neutrophils tended to migrate in "streams" with multiple neutrophils following parallel paths while entering or leaving swarms (Movies S1, S6, and S7). To quantitate this phenomenon, we calculated the angle between the migration trajectories of pairs of cells (alpha) and plotted mean alpha as a function of spatial distance between cells in the pair (Figure 2E). For runs in which swarming was not observed, the mean alpha was close to 90 degrees, consistent with lack of coordinated movement. In contrast, for runs in which swarms formed, alpha was substantially less than 90 degrees, a trend that could be seen even for cell pairs that were > 100 microns apart. This streaming behavior could reflect communication between migrating cells, as been described for swarm formation in *Dictyostelium* (Kriebel et al., 2003) and/or may reflect a common response to competing attractive signals from fluctuating swarm centers.

Neutrophil Swarms Are Initiated by Pioneer Neutrophils and Parasite Egress

To obtain clues about the signals that initiate swarm formation, we carefully examined parasite and neutrophil behavior during each recorded example of swarm formation. In some cases, swarms formed in regions in which no parasites were visible and in absence of any obvious initiating event. However, in 40% (9/22) of swarm initiation events examined, swarm formation occurred in two distinct temporal stages (Figure 3, Figure S2, and Movies S6, S7, S8, and S9). In these examples, the formation of a few "pioneer" neutrophils into a small cluster was followed a few minutes later by large-scale migration of cells into the cluster. Importantly, during the initial phase of swarm formation, some neutrophils could be seen migrating randomly past the swarm center and did not begin their directional migration toward the swarm until several minutes after the arrest of the

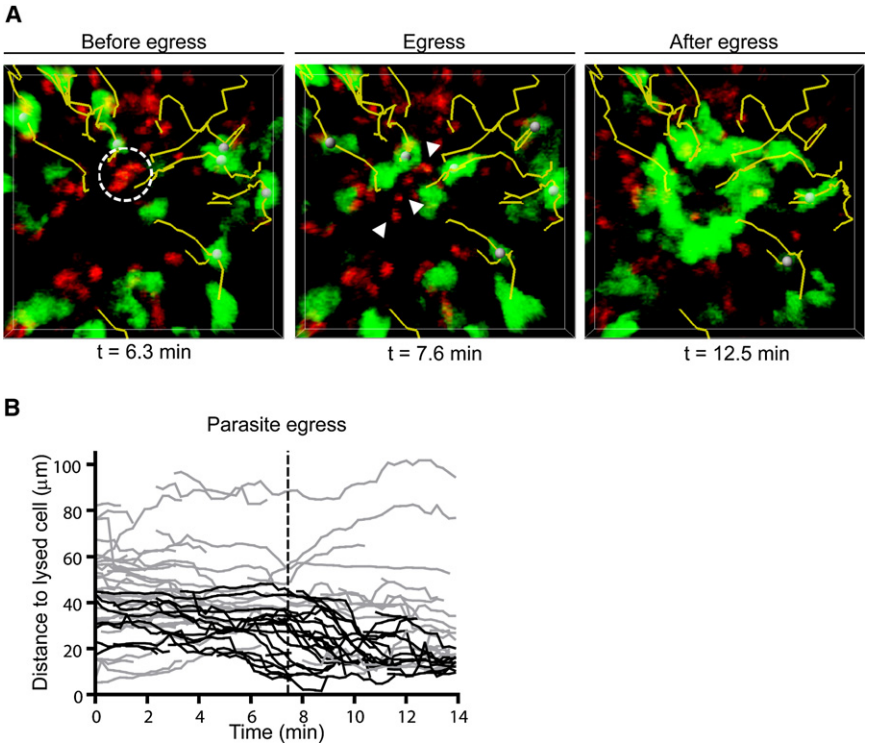

Figure 4. Parasite Egress Coincides with Neutrophil Clustering

Parasite egress is indicated by close apposition of nonmotile parasites and then the sudden acquisition of parasite motility. As shown in (A), neutrophils (lysGFP reporter) are in green and *T. gondii* (RFP) are in red. The tracks of neutrophils that enter cluster are indicated as yellow lines. The left panel shows a time point before parasite egress. The nonmotile group of parasites is indicated by a dashed white circle. The middle panel shows the time point when parasite motility is first detected. Newly motile parasites are indicated by arrowheads. The right panel shows a time point after egress. (B) shows the distance from neutrophil at each time point to the site of parasite egress. Black lines correspond to the tracks of individual cells that migrate toward the site of parasite egress. Shaded lines indicate tracks that do not join the cluster.

pioneer neutrophils (Figure 3, Figure S2, and Movies S6 and S8). This suggests that only the pioneer neutrophils responded to the initial signal and that the late-arriving neutrophils were responding to an amplified signal generated by the pioneers.

Another clue to the initiation of swarm formation came from examination of runs with particularly heavily infected lymph nodes. In these samples, we occasionally observed groups of closely apposed nonmotile parasites that suddenly became motile and migrated rapidly away from the group (Figure 4A, Figure S2A, and Movies S9, S10, and S11). Such behavior is typical for parasite egress from infected cells leading to cell lysis and invasion of neighboring cells (Black and Boothroyd, 2000). Interestingly, egress coincided closely in space and time with the initiation of a swarm in most (4/5) examples observed. The response of neutrophils to parasite egress was extremely rapid, with directed migration detectable at the same time points or even seconds before increased parasite motility was first detectable (Figure 4B and Figure S2B).

Neutrophil Swarms Lead to Removal of Subcapsulary Sinus Macrophages

Because neutrophils are known to degrade tissues by releasing matrix metalloproteinases, the appearance of swarms in the subcapsular sinus of lymph nodes raised the possibility that neutrophil recruitment to lymph nodes during infection could alter lymph-node structure. Indeed we found that, whereas uninfected lymph nodes had a continuous layer of $CD169^+$ macrophages along the lymph-node sinus (Figure 5A, left panels), infected lymph nodes showed gaps in the CD169 staining that often coincided with the location of neutrophil clusters (Figures 5A and 5B, right panels, arrows). We also saw a loss of $CD169^+$ cells by flow-cytometric analysis of infected lymph nodes (Figure S3), suggesting that SCS macrophage did not migrate elsewhere in the lymph node. In vivo depletion of neutrophils prior to infection mostly prevented the appearance of gaps in the layer of $CD169^+$ macrophages, even in regions of the subcapsular sinus that were heavily infected (Figure 5C). Thus although parasite egress also produces some cell lysis, neutrophil swarms, rather than infection per se, were primarily responsible for the gaps in the layer of SCS macrophages reported here. To examine the temporal relationship between swarming and the removal of subcapsular sinus macrophages, we visualized neutrophil migration in real time in samples from lysGFP reporter mice that had been injected with fluorescent $CD169^+$ antibodies along with RFP-labeled parasites (Figure 5D and Movie S12). At the beginning of the run, a continuous region of CD169 staining was visible, and after a few minutes a transient swarm appeared and dissolved, leaving behind a gap in the CD169 staining in the same location as the transient swarm. Because spectral overlap between the GFP from neutrophils can obscure the loss of CD169 staining, we also examined lymph nodes from infected mice in which CD169 cells were labeled but neutrophils were not (Figure 5E and Movie S13). In these samples, we also observed regions of CD169 clearing with a size and rate of appearance that suggested that they coincide with neutrophil swarms. Together, these data indicate that neutrophil swarms lead to the removal of subcapsular sinus macrophages.

Neutrophil Swarming and Removal of Subcapsulary Sinus Macrophages Also Occurred in Lymph Nodes after Oral Infection

To confirm our observations using a more physiological route of infection, we infected LysGFP reporter mice orally with cysts generated from RFP-expressing parasites and examined neutrophil recruitment, localization, and migration in mesenteric lymph nodes. Although few neutrophils were detected in mesenteric lymph nodes of uninfected mice, neutrophils (GFP^{hi} $Ly6G^+$)

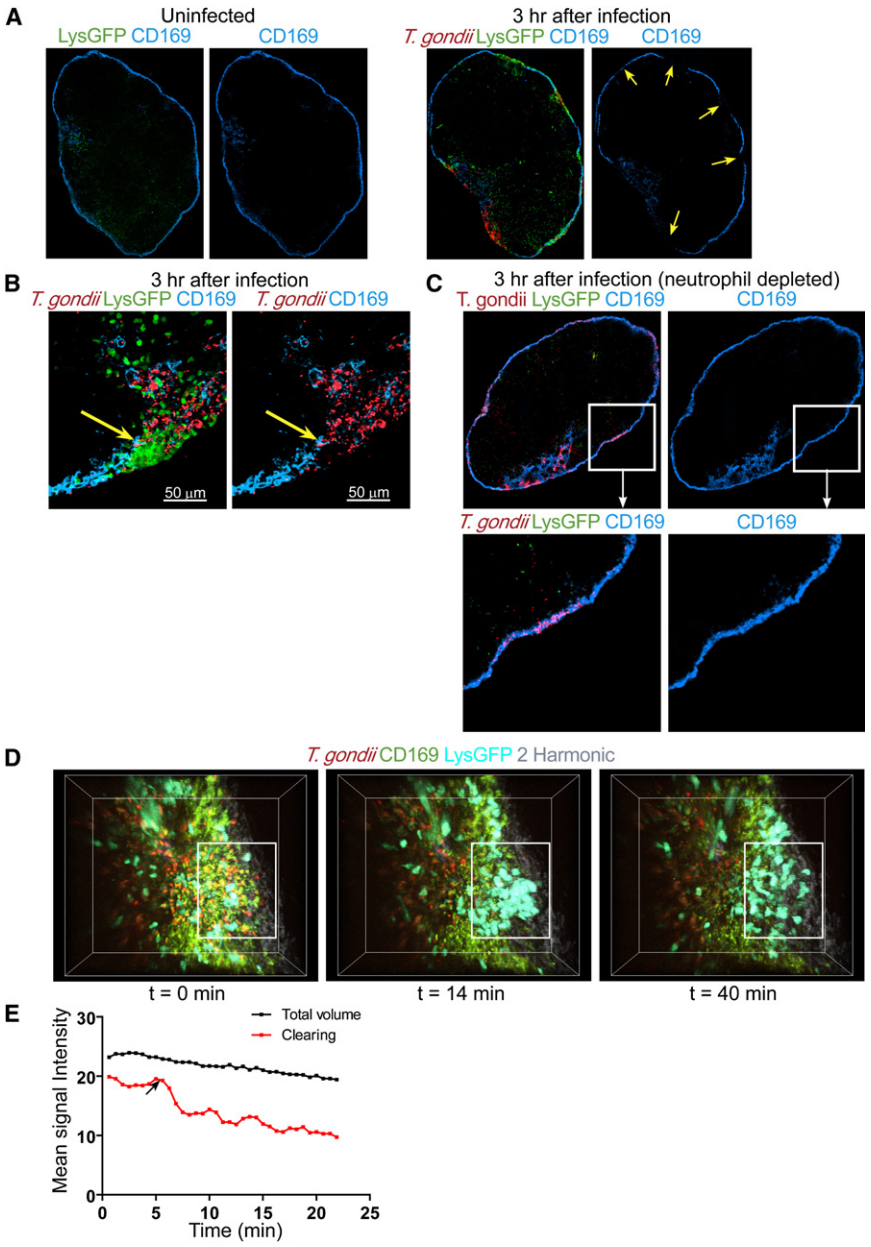

Figure 5. Neutrophil Clearing of CD169$^+$ Macrophages

(A) Low-magnification confocal images of a whole lymph node of LysGFP reporter (green) stained with CD169 antibody (blue). The left pair of panels shows an uninfected lymph node, whereas the right pair shows a draining lymph node 3 hr after infection with RFP parasites (red). Right-hand panels of each group show CD169 staining only. Yellow arrows indicate location of gaps in the CD169 staining.

(B) Higher-magnification confocal image of a lymph-node section showing a neutrophil cluster (green) in an area free of parasites (red) and CD169 staining (blue). The right panel shows CD169 and parasite signal only. The position of swarm is indicated by yellow arrows.

(C) Confocal image of a draining lymph node from a mouse that was depleted of neutrophils just prior to infection and analyzed 3 hr after infection with RFP parasites. The lower panels show an enlarged view of the boxed area indicating an area of high infection within a continuous CD169 layer. Right panels show CD169 staining only.

(D) Two-photon images of a lymph node showing CD169 staining (green), neutrophils (cyan), parasites (red), and lymph-node capsule (second harmonic signal in gray). The left panel shows a time point just before a swarm forms. The middle panel shows a time point during swarming. The cleared area is indicated by a white rectangle. The right panel shows a time point just after the swarm breaks up.

(E) Progressive disappearance of CD169 signal in local region of lymph-node sinus. Fluorescence intensity of CD169 labeling in an area where clearing was observed by two-photon imaging and plotted against time (red line). The change in fluorescence intensity for the whole imaging volume is shown as a control for fluorophore bleaching (black line). Arrow indicates the approximate time when CD169 clearing was first observed.

were readily detectable by day 4–5 after oral infection (Figures 6A and 6B). Neutrophils formed clusters throughout the lymph nodes of infected mice, including some near the subcapsular sinus (Figure 6B, white arrows). TPSLM of intact mesenteric lymph nodes revealed migration dynamics of reporter positive cells similar to that observed in draining lymph nodes after earflap infection (Movie S14). Moreover, we also detected gaps in the layer of CD169$^+$ SCS macrophage in mesenteric lymph nodes of infected mice, and these often coincided with the location of clusters of reporter-positive cells (Figure 6C, white arrow). It is noteworthy that, although parasites and neutrophils were concentrated at the SCS of draining lymph nodes after earflap infection, parasites and neutrophils were found both in the SCS and in deeper regions of the mesenteric lymph node after oral infection. This is likely to reflect the less synchronous arrival of parasites in mesenteric lymph nodes after oral infection compared to earflap infection. Nevertheless, these results confirm that the recruitment and behavior of neutrophil in the SCS of the lymph node described here are not unique to the earflap infection model but also occur after oral infection with *T. gondii*.

DISCUSSION

In addition to their well-characterized role in infected tissues, recent evidence indicates that neutrophils also play important roles in immune responses within lymph nodes. Here, we provide the first report of the dynamics of neutrophil behavior in intact lymph nodes in the setting of *Toxoplasma gondii* infection. We showed that neutrophils migrate in a distinctive, coordinated fashion that leads to the formation of swarms near sites of infection at the subcapsular sinus of draining lymph nodes. We showed that neutrophil swarms can be initiated by the cooperative action of neutrophils, as well as by parasite egress from host

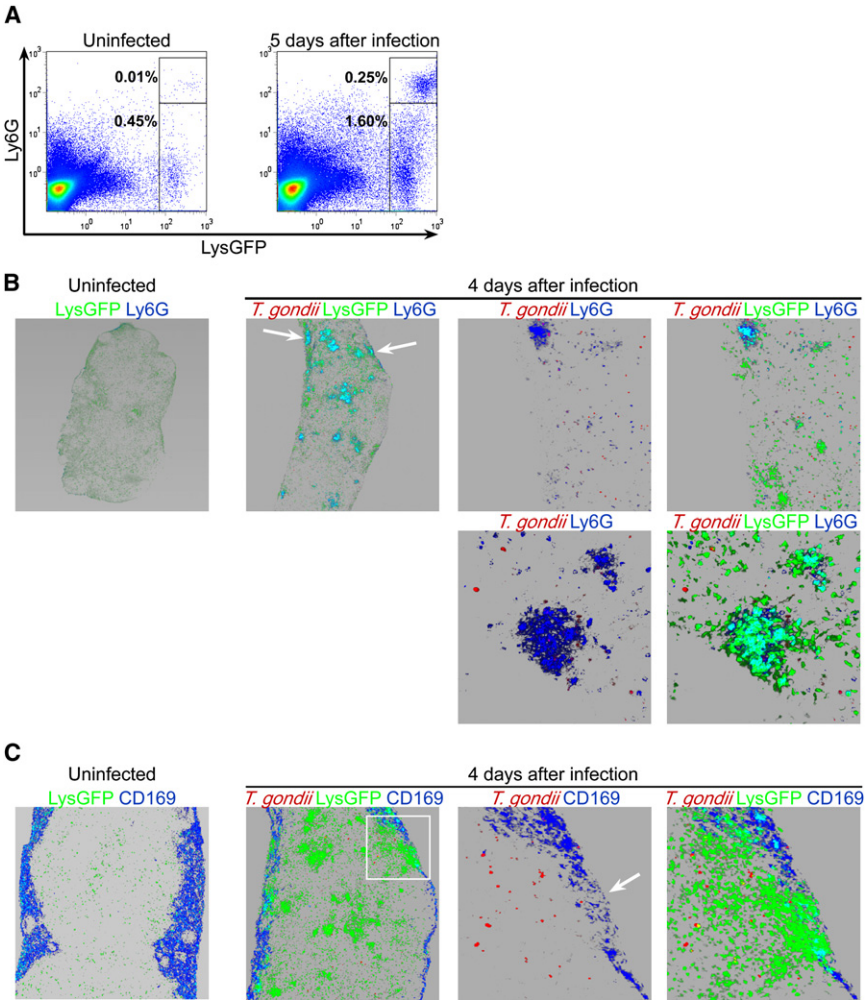

Figure 6. Neutrophil Recruitment and Swarm Formation in Mesenteric Lymph Nodes after Oral Infection

(A) Neutrophils (LysGFP^{hi}Ly6G^{+}) in the mesenteric lymph nodes of orally infected mice. Flow-cytometric analysis of mesenteric lymph nodes of uninfected LysGFP mice, or LysGFP reporter mice infected 5 days earlier with 20 cysts.

(B) Shown are 20 um frozen sections of mesenteric lymph nodes of LysGFP reporter (green) mice before infection (left panel) or 4 days after oral infection with 45 cysts of Pruniaud-RFP (red) stained with Ly6G (blue). Arrows indicate neutrophil cluster at the subcapsulary sinus. Bottom panels show a high-magnification image of a lymph node from an infected mouse. Clusters of LysGFP high cells (green) (left panel) stain positive for the neutrophil marker Ly6G (blue).

(C) We stained the same samples as in (B) to visualize CD169^{+} subcapsular sinus macrophages (blue). A panel on the right shows a high-magnification image with an arrow indicating a region of CD169 clearing.

cells, and that neutrophil swarms lead to the removal of macrophages that line the subcapsular sinus of the lymph nodes. Our data provide a new perspective for future studies on the role of neutrophils in lymph nodes.

Perhaps the most striking feature of neutrophil behavior reported here is the highly cooperative nature of their migration patterns. This is reflected in the ''paparazzi-like'' behavior of neutrophils in which the initial arrest of a small number of neutrophils was followed minutes later by a massive influx of cells. This behavior is likely to be mediated by multiple chemoattractants including CXCL8 (IL-8), CXCL1, and leukotriene B4, which are both produced by, and attractive to, neutrophils (Baggiolini, 1998; Scapini et al., 2000). The cooperative nature of neutrophil migration is also reflected in their streaming behavior during swarm formation, which is reminiscent of swarm formation by the slime mold *Dictyostelium*. In the case of *Dictyostelium,* evidence suggests that individual cells leave trails of chemoattractants that are sensed by neighboring cells, leading to a head-to-tail migration pattern as cells migrate toward a swarm (Kriebel et al., 2003). Neutrophils and *Dictyostelium* appear to use similar signal transduction systems for chemoattraction (Mahadeo et al., 2007) and it will be interesting to explore whether similar mechanisms also underlie their co-operative migration patterns.

Another indication of cooperative action of neutrophils in swarm formation is correlation between the size and persistence of neutrophil swarms. Swarms containing fewer than 150 neutrophils tended to be transient, with neutrophils migrating rapidly and directionally toward swarm center, and then migrating equally rapidly out of the swarm to nearby join neighboring growing swarm centers. In contrast, swarms with > 300 neutrophils invariably kept growing over the time they were observed, often merging with nearby swarms. Although it is likely that persistent swarms would disappear eventually in vivo, this would likely result from neutrophil apoptosis and phagocytosis by macrophages, in contrast to the outward migration of neutrophils seen during the dissolution of transient swarms. The correlation between size and persistence strongly suggests that the neutrophils themselves contribute to the gradient of chemoattractants that generates a swarm, and that once the swarm reaches a certain size, these signals become sufficiently strong to generate a stable swarm center that can override other competing signals in the environment.

Another striking aspect of neutrophil behavior is their extremely rapid migration toward sites of parasite egress. Because this response occurred within seconds of parasite egress, it is unlikely to be related to the IL-1-dependent neutrophil recruitment in response to dying cells has been characterized previously (Chen et al., 2007). Although the nature of the neutrophil-attracting signal that correlates with parasite egress is unclear, it is possible that material from lysed cells could be directly attractive for neutrophils, a phenomenon termed ''necrotaxis'' that has been previously described in vitro (Debru, 1993). Alternatively, the released parasites themselves could attract neutrophils, either because of a direct response to parasite PAMPS (Debierre-Grockiego et al., 2007; Nakao and Konishi, 1991a;

Yarovinsky et al., 2005) or because of limited complement activation by parasites (Fuhrman and Joiner, 1989). An in vitro system to recapitulate neutrophil swarming in response to *Toxoplasma* infection would help to address these possibilities.

Given the multitude of signals known to attract neutrophils, and the indications from our data that neutrophils are responding to multiple, competing signals, it seems likely that many different types of chemoattractants contribute to neutrophil swarming behavior. It is unlikely that adaptive immunity plays a major role in the neutrophil behavior that we report here because these responses occurred in naive mice a few hours after exposure to the parasites, time points well before T or B cells would be expected to be activated. Moreover, we have not observed any significant differences in neutrophil behavior in immunized versus naive mice (data not shown). One major challenge to identify these signals will be to selectively block candidate signals during the swarming phase of the response. For example, while TLR-MyD88 signals are good candidates for mediating swarm formation, our observation that this pathway is also required for neutrophils to be recruited to the lymph node in the first place complicates testing this idea.

Our data also add to the growing body of evidence for the importance of $CD169^+$ subcapsular sinus macrophage of the lymph nodes (Carrasco and Batista, 2007; Hickman et al., 2008; Junt et al., 2007; Phan et al., 2007). Parasites are found predominantly within these macrophage a few hours after infection, and neutrophil swarms in infected regions of the subcapsular sinus lead to the appearance of gaps in the layer of $CD169^+$ cells, which normally form a continuous layer around an uninfected lymph node. Although the fate of the SCS macrophages is not known, we suspect that they are removed by neutrophils on the basis of several considerations. First, we have never observed any migrating $CD169^+$ macrophages, even while imaging areas in which gaps were forming. Second, we are able to detect the loss of $CD169^+$ cells by flow-cytometric analysis, consistent with the removal of these cells and arguing against the possibility that they have migrated to a different part of the lymph node. Finally, a direct role for neutrophils is supported by the well-documented ability of neutrophils to produce matrix metalloproteases and participate in tissue remodeling. Regardless of the mechanism, given the emerging evidence for the importance of subcapsular sinus of the lymph node in trapping pathogens and initiating adaptive immune responses (Carrasco and Batista, 2007; Hickman et al., 2008; Junt et al., 2007; Phan et al., 2007), it will be important to examine whether the removal of SCS macrophage by neutrophils has an impact on subsequent immune responses.

In summary, our analysis of neutrophil migration in intact lymph nodes has provided evidence that signals released during parasite egress from host cells and cooperative action of neutrophils can induce the formation of dynamic neutrophil swarms in the SCS, leading to the removal of macrophages that reside there. In addition to direct phagocytic killing, neutrophils also use a variety of other non-cell-autonomous mechanisms to protect against pathogens, including the release of neutrophil extracellular traps (NETs) (Brinkmann et al., 2004), containing DNA, microbiocidal products, and tissue remodeling factors such as matrix metalloproteinase (Appelberg, 2007; Nathan, 2006). It is tempting to speculate that the swarming behavior of neutrophils reported here could increase the local concentration of these released products and improve the effectiveness of these mechanisms to induce inflammation and provide protection against pathogens.

EXPERIMENTAL PROCEDURES

Mice

All mice were bred and housed in pathogen-free conditions at the AALAC-approved animal facility at Life Science Addition, University of California, Berkeley. All animal experiments were approved by the Animal Care and Use Committee of UC Berkeley. LysGFP reporter mice were a gift from T. Graf (Albert Einstein College of Medicine, Bronx, NY) and have been previously described (Faust et al., 2000). *MyD88* gene KO mice (originally generated in S. Akira's laboratory, Osaka University, Osaka, Japan) (Adachi et al., 1998) were backcrossed onto C57BL/6 background.

Parasites

To generate a *T. gondii* cell line expressing the tandem (td) Tomato variant of red fluorescent protein (RFP) (Shaner et al., 2004), we amplified tdTomato using the primers 5′-AGTCCCTAGGGTGAGCAAGGGCGAGGAG-3′ and 5′-AGTCCCCGGGCTTGTACAGCTCGTCCATGC-3′. We digested the resultant PCR product with AvrII and XmaI and ligated this into the corresponding restriction enzyme sites of the pCTG vector (G.v.D. and R. Opperman, unpublished data) to generate the vector $pCTR_{2T}$, in which expression of cytosol-localized tdTomato is driven from the constitutive α-tubulin promoter. We transfected this construct into the RHΔhxgprt strain of *T. gondii* and generated stable lines expressing tdTomato by chloramphenicol selection as previously described (Gubbels et al., 2005). In brief, 1×10^7 parasites were resuspended in cytomix containing 50 μg of linearized $pCTR_{2T}$ vector. The parasites mixture was added to a 2 mm electroporation cuvette and electroporated with a BTX ECM 630 electroporator at 1500 V, 25 Ω, and 25 μF. Transfected cells were passed onto fresh host cells. Chloramphenicol was added to a final concentration of 6.8 μg/mL 16 hr after transfection. Cells were passaged in the presence of chloramphenicol until stable lines were generated. Clonal lines of the RH/tdTomato parasite strain were obtained by fluorescence-activated cell sorting. In brief, parasites were filtered through a 3 μm filter, pelleted, and resuspend in phosphate-buffered saline. Parasites were sorted with a MoFlo cytometer (Dako, Ft Collins, CO) with an Enterprise 631 laser tuned to 488 nm for excitation and an emission filter with a band pass of 570/40 nm. Bright parasites were sorted into 96-well plates, and wells containing single plaques after 1 week of growth were considered to consist of a clonal parasite line. All parasites were maintained in confluent human foreskin fibroblasts.

For mouse infections, parasites were prepared from almost fully lysed fibroblast cultures by first releasing the parasites from fibroblasts by passing them through 21 G1 1/2 gauge and 23 G1 needles five to ten times. Parasites were then filtered through a 3 μm filter, pelleted, and resuspended in phosphate-buffered saline. A total of 5×10^5 to 1×10^7 parasites (typically 5×10^6) in 10 μl volume were injected into the earflap. No differences in the anatomical distribution of parasites or neutrophils in draining lymph nodes were observed over this range of infection. Some of the mice used for two-photon experiments were injected with 10^6 irradiated parasites intraperitoneally at least 4 weeks prior to infection and imaging. No differences in neutrophil behavior were observed between immunized and naive animals. For neutrophil depletion experiments, mice were injected i.p. with 1 mg of Ly6G antibody (clone 1A8) 2 days prior to infection and also i.v. with 0.5 mg of Ly6G antibody 1 day prior to infection.

For oral infections, Prugnaud-RFP parasites were engineered essentially as described above for RH parasites, and cysts were isolated from brain homogenates of CBA/J mice (Jackson Laboratory) infected with 300–400 parasites i.p. 4–6 months prior. Cysts were counted after staining with Dolichos Biflorus Agglutinin (Vector Laboratories). LysGFP reporter mice were infected with 20–45 cysts by gavage. Mesenteric lymph nodes were used for microscopy or analyzed by flow cytometry.

Antibodies and Flow Cytometry

Lymph nodes were dissociated by collagenase digestion. Cell suspensions were filtered, stained, and analyzed by flow cytometry. The following

antibodies were from eBioscience: phycoerythrin-Cy5 conjugated anti-CD11b (clone M1/70) and phycoerythrin-Cy5 conjugated anti-CD11c (clone N418). Fluorescein-isothiocyanate-conjugated anti-Ly6G (clone 1A8) was from BD Biosciences. Fluorescein-isothiocyanate-conjugated CD169 antibody (clone 3D6.112) was purchased from AbD Serotec. Acquisitions were performed with a Coulter Epics XL-MCL flow cytometer (Beckman-Coulter), and data were analyzed with the FlowJo software (Tree Star).

Statistical Analysis

Values were expressed as mean ± standard error (SE). Levels of significance were calculated by unpaired t tests with the GraphPad Prism program. Differences were considered significant at $p < 0.05$.

Two-Photon Imaging

One to five hours after ear-flap injection, mice were sacrificed, and dorsal cervical (draining) lymph nodes were isolated and imaged by two-photon laser scanning microscopy (TPLSM) while being perfused with warmed, oxygenated medium as described previously (Witt et al., 2005). Imaging was performed on either upright Zeiss NLO 510 or a custom-built microscope, both using a Spectra-Physics MaiTai laser tuned to 900–920nm. For the Zeiss microscope, GFP and tdTomato emission light was separated with a 560 dichroic mirror and collected with non-descanned detectors. For the custom-built microscope, the emission light was separated with 495 and 560 dichroics and collected with 3 PMT detectors. Bandpass filters HQ 450/80M and HQ 645/75M were used for minimization of spectral overlap.

Typical imaging volumes (164 × 164 × 40 μm or 172 × 143 × 80 μm, respectively) corresponded to regions of the lymph nodes extending up to 200 μm below the surface of the capsule and were scanned every 13–37 s for 20–40 min. Mesenteric lymph nodes were imaged under similar conditions 4–5 days after oral infection.

Data Analysis

The x, y, z coordinates of individual cells over time were obtained with Imaris Bitplane Software. Motility parameters were calculated with Matlab (code available upon request). Parameters reported here include speed (defined as path length over time; μm/minute) and distance to swarm center (μm). For measurement of the volumes of individual neutrophil swarms, isosurfaces were generated in the GFP channel (threshold of 130, 6 μm Gaussian filter), and the volume of each isosurface was determined over time. The volume of a single neutrophil was estimated with the same method (with 1 μm Gaussian filter), and 15 individual cell volumes were averaged. For analysis of directed migration, psi is defined as the angle between the migration vector and the direction vector from the initial position of the migrating cell to the center of the swarm (see inset, Figure 2D). The "coordination angle" alpha is defined as the angle between the migration vectors for pairs of time points within two individual tracks (see inset, Figure 2E).

Immunofluorescence

Isolated lymph nodes were fixed with 4% formalin/10% sucrose in PBS for 1 hr, sequentially submerged in 10%, 20%, and 30% sucrose for 18–24 hr each, and frozen over dry ice in OCT. We generated 20 psi serial sections by cryosectioning (MICROM H550, Microm GmbH) and stored them at −80°C. Sections were brought to room temperature, fixed with cold acetone for 10 min, air-dried, and incubated with 10% mouse serum in Fc blocking reagent (2.4G2 culture supernatant) for 1 hr. The tissue was stained with unconjugated anti-Ly6G (BD Biosciences), purified rat anti mouse CD169 (AbD Serotec), or biotin-conjugated anti-LYVE-1 (R&D Systems) overnight at 4°C. After primary staining, slides were washed 4× in PBS and incubated with either anti-rat Alexa 647 or streptavidin Alexa 633 (Invitrogen) for 2 hr at room temperature. Sections were then washed 4× in PBS and coverslipped with VectaShield (Vector Laboratories) mounting medium. Stained lymph-node sections were visualized on Zeiss 510 Axioplan META NLO upright microscope with a 10× air objective (Plan-Neofluar 10×/0.3) and a 40× oil objective (Plan-Neofluar 40×/1.3 oil WD = 0.17 mm) with 488 nm, 543 nm, and 633 nm laser lines. Images were analyzed and assembled with Adobe Photoshop and Imaris Bitplane.

SUPPLEMENTAL DATA

Supplemental Data include three figures and fourteen movies and can be found with this article online at http://www.immunity.com/cgi/content/full/29/3/487/DC1/.

ACKNOWLEDGMENTS

We thank H. Nolla (UCB) and J. Nelson (CTEGD) for assistance with flow cytometry, M. Rivera for flow-cytometry analysis, T. Graf for providing lysMGFP reporter mice, Y.F. Liao for tracking neutrophils, E. Ladi for assistance with quantitating neutrophil motility, the CHPS mouse/virus core for providing mouse strains, and D. Portnoy, M. Welsh, and members of the Robey lab for comments on the manuscript. This work was funded by the NIH (B.S. and E.R.), Human Frontier Science Program Fellowship (T.C.), and C.J. Martin Overseas Fellowship (400489) from the Australian National Health and Medical Research Council (G.v.D.).

Received: June 14, 2008
Revised: July 18, 2008
Accepted: July 25, 2008
Published online: August 21, 2008

REFERENCES

Abadie, V., Badell, E., Douillard, P., Ensergueix, D., Leenen, P.J., Tanguy, M., Fiette, L., Saeland, S., Gicquel, B., and Winter, N. (2005). Neutrophils rapidly migrate via lymphatics after Mycobacterium bovis BCG intradermal vaccination and shuttle live bacilli to the draining lymph nodes. Blood *106*, 1843–1850.

Adachi, O., Kawai, T., Takeda, K., Matsumoto, M., Tsutsui, H., Sakagami, M., Nakanishi, K., and Akira, S. (1998). Targeted disruption of the MyD88 gene results in loss of IL-1- and IL-18-mediated function. Immunity *9*, 143–150.

Appelberg, R. (2007). Neutrophils and intracellular pathogens: Beyond phagocytosis and killing. Trends Microbiol. *15*, 87–92.

Baggiolini, M. (1998). Chemokines and leukocyte traffic. Nature *392*, 565–568.

Beauvillain, C., Delneste, Y., Scotet, M., Peres, A., Gascan, H., Guermonprez, P., Barnaba, V., and Jeannin, P. (2007). Neutrophils efficiently cross-prime naive T cells in vivo. Blood *110*, 2965–2973.

Bennouna, S., Bliss, S.K., Curiel, T.J., and Denkers, E.Y. (2003). Cross-talk in the innate immune system: Neutrophils instruct recruitment and activation of dendritic cells during microbial infection. J. Immunol. *171*, 6052–6058.

Black, M.W., and Boothroyd, J.C. (2000). Lytic cycle of Toxoplasma gondii. Microbiol. Mol. Biol. Rev. *64*, 607–623.

Bliss, S.K., Gavrilescu, L.C., Alcaraz, A., and Denkers, E.Y. (2001). Neutrophil depletion during Toxoplasma gondii infection leads to impaired immunity and lethal systemic pathology. Infect. Immun. *69*, 4898–4905.

Bousso, P., and Robey, E. (2004). Dynamic behavior of T cells and thymocytes in lymphoid organs as revealed by 2-photon microscopy. Immunity *21*, 349–355.

Brinkmann, V., Reichard, U., Goosmann, C., Fauler, B., Uhlemann, Y., Weiss, D.S., Weinrauch, Y., and Zychlinsky, A. (2004). Neutrophil extracellular traps kill bacteria. Science *303*, 1532–1535.

Cahalan, M.D., and Parker, I. (2008). Choreography of cell motility and interaction dynamics imaged by two-photon microscopy in lymphoid organs. Annu. Rev. Immunol. *26*, 585–626.

Carrasco, Y.R., and Batista, F.D. (2007). B cells acquire particulate antigen in a macrophage-rich area at the boundary between the follicle and the subcapsular sinus of the lymph node. Immunity *27*, 160–171.

Channon, J.Y., Seguin, R.M., and Kasper, L.H. (2000). Differential infectivity and division of Toxoplasma gondii in human peripheral blood leukocytes. Infect. Immun. *68*, 4822–4826.

Chen, C.J., Kono, H., Golenbock, D., Reed, G., Akira, S., and Rock, K.L. (2007). Identification of a key pathway required for the sterile inflammatory response triggered by dying cells. Nat. Med. *13*, 851–856.

Debierre-Grockiego, F., Campos, M.A., Azzouz, N., Schmidt, J., Bieker, U., Resende, M.G., Mansur, D.S., Weingart, R., Schmidt, R.R., Golenbock, D.T., et al. (2007). Activation of TLR2 and TLR4 by glycosylphosphatidylinositols derived from Toxoplasma gondii. J. Immunol. *179*, 1129–1137.

Debru, C. (1993). A particular form of chemotaxis: Necrotaxis. An historical view. Blood Cells *19*, 5–19.

Denkers, E.Y., Butcher, B.A., Del Rio, L., and Bennouna, S. (2004). Neutrophils, dendritic cells and Toxoplasma. Int. J. Parasitol. *34*, 411–421.

Egen, J.G., Rothfuchs, A.G., Feng, C.G., Winter, N., Sher, A., and Germain, R.N. (2008). Macrophage and T cell dynamics during the development and disintegration of mycobacterial granulomas. Immunity *28*, 271–284.

Faust, N., Varas, F., Kelly, L.M., Heck, S., and Graf, T. (2000). Insertion of enhanced green fluorescent protein into the lysozyme gene creates mice with green fluorescent granulocytes and macrophages. Blood *96*, 719–726.

Fuhrman, S.A., and Joiner, K.A. (1989). Toxoplasma gondii: Mechanism of resistance to complement-mediated killing. J. Immunol. *142*, 940–947.

Germain, R.N., Miller, M.J., Dustin, M.L., and Nussenzweig, M.C. (2006). Dynamic imaging of the immune system: Progress, pitfalls and promise. Nat. Rev. Immunol. *6*, 497–507.

Gubbels, M.J., Striepen, B., Shastri, N., Turkoz, M., and Robey, E.A. (2005). Class I major histocompatibility complex presentation of antigens that escape from the parasitophorous vacuole of Toxoplasma gondii. Infect. Immun. *73*, 703–711.

Hickman, H.D., Takeda, K., Skon, C.N., Murray, F.R., Hensley, S.E., Loomis, J., Barber, G.N., Bennink, J.R., and Yewdell, J.W. (2008). Direct priming of antiviral CD8+ T cells in the peripheral interfollicular region of lymph nodes. Nat. Immunol. *9*, 155–165.

Junt, T., Moseman, E.A., Iannacone, M., Massberg, S., Lang, P.A., Boes, M., Fink, K., Henrickson, S.E., Shayakhmetov, D.M., Di Paolo, N.C., et al. (2007). Subcapsular sinus macrophages in lymph nodes clear lymph-borne viruses and present them to antiviral B cells. Nature *450*, 110–114.

Kriebel, P.W., Barr, V.A., and Parent, C.A. (2003). Adenylyl cyclase localization regulates streaming during chemotaxis. Cell *112*, 549–560.

Mahadeo, D.C., Janka-Junttila, M., Smoot, R.L., Roselova, P., and Parent, C.A. (2007). A chemoattractant-mediated Gi-coupled pathway activates adenylyl cyclase in human neutrophils. Mol. Biol. Cell *18*, 512–522.

Maletto, B.A., Ropolo, A.S., Alignani, D.O., Liscovsky, M.V., Ranocchia, R.P., Moron, V.G., and Pistoresi-Palencia, M.C. (2006). Presence of neutrophil-bearing antigen in lymphoid organs of immune mice. Blood *108*, 3094–3102.

Megiovanni, A.M., Sanchez, F., Robledo-Sarmiento, M., Morel, C., Gluckman, J.C., and Boudaly, S. (2006). Polymorphonuclear neutrophils deliver activation signals and antigenic molecules to dendritic cells: A new link between leukocytes upstream of T lymphocytes. J. Leukoc. Biol. *79*, 977–988.

Miller, M.J., Wei, S.H., Parker, I., and Cahalan, M.D. (2002). Two-photon imaging of lymphocyte motility and antigen response in intact lymph node. Science *296*, 1869–1873.

Nakao, M., and Konishi, E. (1991a). Neutrophil chemotactic factors secreted from Toxoplasma gondii. Parasitology *103*, 29–34.

Nakao, M., and Konishi, E. (1991b). Proliferation of Toxoplasma gondii in human neutrophils in vitro. Parasitology *103*, 23–27.

Nathan, C. (2006). Neutrophils and immunity: Challenges and opportunities. Nat. Rev. Immunol. *6*, 173–182.

Pesce, J.T., Liu, Z., Hamed, H., Alem, F., Whitmire, J., Lin, H., Liu, Q., Urban, J.F., Jr., and Gause, W.C. (2008). Neutrophils clear bacteria associated with parasitic nematodes augmenting the development of an effective th2-type response. J. Immunol. *180*, 464–474.

Phan, T.G., Grigorova, I., Okada, T., and Cyster, J.G. (2007). Subcapsular encounter and complement-dependent transport of immune complexes by lymph node B cells. Nat. Immunol. *8*, 992–1000.

Rydstrom, A., and Wick, M.J. (2007). Monocyte recruitment, activation, and function in the gut-associated lymphoid tissue during oral Salmonella infection. J. Immunol. *178*, 5789–5801.

Sasmono, R.T., Ehrnsperger, A., Cronau, S.L., Ravasi, T., Kandane, R., Hickey, M.J., Cook, A.D., Himes, S.R., Hamilton, J.A., and Hume, D.A. (2007). Mouse neutrophilic granulocytes express mRNA encoding the macrophage colony-stimulating factor receptor (CSF-1R) as well as many other macrophage-specific transcripts and can transdifferentiate into macrophages in vitro in response to CSF-1. J. Leukoc. Biol. *82*, 111–123.

Sayles, P.C., and Johnson, L.L. (1996). Exacerbation of toxoplasmosis in neutrophil-depleted mice. Nat. Immun. *15*, 249–258.

Scapini, P., Lapinet-Vera, J.A., Gasperini, S., Calzetti, F., Bazzoni, F., and Cassatella, M.A. (2000). The neutrophil as a cellular source of chemokines. Immunol. Rev. *177*, 195–203.

Shaner, N.C., Campbell, R.E., Steinbach, P.A., Giepmans, B.N., Palmer, A.E., and Tsien, R.Y. (2004). Improved monomeric red, orange and yellow fluorescent proteins derived from Discosoma sp. red fluorescent protein. Nat. Biotechnol. *22*, 1567–1572.

Sumen, C., Mempel, T.R., Mazo, I.B., and von Andrian, U.H. (2004). Intravital microscopy: Visualizing immunity in context. Immunity *21*, 315–329.

Tvinnereim, A.R., Hamilton, S.E., and Harty, J.T. (2004). Neutrophil involvement in cross-priming CD8+ T cell responses to bacterial antigens. J. Immunol. *173*, 1994–2002.

Witt, C.M., Raychaudhuri, S., Schaefer, B., Chakraborty, A.K., and Robey, E.A. (2005). Directed migration of positively Selected thymocytes visualized in real time. PLoS Biol. *3*, e160.

Yarovinsky, F., Zhang, D., Andersen, J.F., Bannenberg, G.L., Serhan, C.N., Hayden, M.S., Hieny, S., Sutterwala, F.S., Flavell, R.A., Ghosh, S., and Sher, A. (2005). TLR11 activation of dendritic cells by a protozoan profilin-like protein. Science *308*, 1626–1629.

Zinselmeyer, B.H., Lynch, J.N., Zhang, X., Aoshi, T., and Miller, M.J. (2008). Video-rate two-photon imaging of mouse footpad - a promising model for studying leukocyte recruitment dynamics during inflammation. Inflamm. Res. *57*, 93–96.